Available online at www.sciencedirect.com
SCIENCE DIRECT®
Chemical Physics Letters 388 (2004) 94–99
CHEMICAL PHYSICS LETTERS
www.elsevier.com/locate/cplett

Direct ab initio dynamics studies of the reactions of HNO with H and OH radicals

Hue Minh Thi Nguyen [a,b,1], Shaowen Zhang [a], Jozef Peeters [b], Thanh N. Truong [a,*], Minh Tho Nguyen [b,*]

[a] *Henry Eyring Center for Theoretical Chemistry, Department of Chemistry, University of Utah, Salt Lake City, UT 84112, USA*
[b] *Department of Chemistry, University of Leuven, Celestijnenlaan 200F, B-3001 Leuven, Belgium*

Received 18 January 2004; in final form 2 March 2004
Published online: 18 March 2004

Abstract

Ab initio calculations using the UMP2 and UQCISD methods with correlation consistent double-zeta and triple-zeta basis sets were applied to study the reactions of HNO with H and OH radicals. The classical energy barrier for the abstraction $H + HNO \rightarrow H_2 + NO$ is 0.5 kcal/mol. The reaction path of $OH + HNO$ is: $OH + HNO \rightarrow$ HNO(OH)-complex $\rightarrow$ TS $\rightarrow$ NO(H_2O)-complex $\rightarrow H_2O + NO$ with no energy barrier relative to $OH + HNO$ entrance channel. Canonical and microcanonical variational transition state theory calculations were carried out for these reactions (200–2500 K) and compared with available experimental kinetic data.

1. Introduction

The reactions between HNO with atomic hydrogen and hydroxyl radicals:

$$HNO + H \rightarrow H_2 + NO \quad (1)$$

$$HNO + OH \rightarrow H_2O + NO \quad (2)$$

are known to account for the NO formation in fuel-rich flames of compounds containing hydrogen, oxygen and nitrogen [1–7]. Due to the importance in modeling NO formation in combustion systems, accurate kinetic information of these reactions is critical. Unfortunately, kinetic data from both experimental and theoretical studies for these reactions in the existing literature are not consistent.

Experimentally, there have been several measurements of the rate constants for these reactions but the reported values were scattered [1,8–12]. There have also been a few theoretical studies reported for the HNO + H reaction. Walch [14] reported the classical barrier for this reaction to be about 0.3 kcal/mol from single-point ICCI/cc-pvTZ calculations using CASSCF(11,9)/cc-pvDZ optimized geometries. Thermal rate constants were predicted by Soto et al. [13] using canonical variational transition state theory (CVT) with the minimum energy path (MEP) information calculated at the CISD/cc-pVDZ//CASSCF/cc-pvDZ level of theory. The classical barrier was found to be 0.99 kcal/mol. The calculated rate constants, however, are considerably faster than the experimental data. Sumathy et al. [15] mapped out the [H_2NO] potential energy surface at the CCSD(T)/6-311++G(3df,3pd)//CCSD(T)/6-311++G(d,p) level of theory. The calculated barrier for the direct H abstraction was reported to be 0.2 kcal/mol. At 2000 K, the calculated rate constant is roughly a factor of 14 times greater than that measured previously by Halstead et al. [8].

To the best of our knowledge, there has been only one theoretical study on the reaction of OH with HNO by Soto et al. [13]. The MEP was calculated at the MRCI/cc-pVDZ//CASSCF(5,5)/cc-pcDZ level of theory. The reaction barrier is predicted to be about 2.0 kcal/mol.

* Corresponding authors. Fax: 321-632-7992 (M.T. Nguyen).
E-mail addresses: truong@chemistry.chem.utah.edu (T.N. Truong), minh.nguyen@chem.kuleuven.ac.be (M.T. Nguyen).
[1] On leave from Faculty of Chemistry, University of Education, Hanoi, Vietnam.

0009-2614/$ - see front matter © 2004 Elsevier B.V. All rights reserved.
doi:10.1016/j.cplett.2004.03.005

The calculated rate constants agree with experimental data from Halstead et al. [8] at 2000 K but are considerably lower than those from Bulewicz et al. [1]. It is interesting to note that from Soto et al. [13] calculations, the barrier height of 0.99 kcal/mol for the H + HNO and of 2.0 kcal/mol for the OH + HNO reaction indicates that the H atom is somewhat more reactive than the OH radical in abstracting hydrogen from HNO. However, it is well known that the OH radical is more reactive than the H atom for abstracting hydrogen from hydrocarbon molecules. These differences warrant the need for further study in particular on the kinetics of the hydrogen abstraction of HNO by H and OH radicals.

In this study, we have carried out direct ab initio dynamics study [16] on the abstraction rates of the reactions $H + HNO \rightarrow H_2 + NO$ and $OH + HNO \rightarrow H_2O + NO$. Thermal rate constants of these reactions were computed by applying the CVT and microcanonical variational transition state theory (μVT) with potential energy surfaces calculated from an accurate level of molecular orbital theory.

2. Computational methods

2.1. Electronic structure calculations

The free radical species, such as those involved in the H + HNO and OH + HNO reactions, are usually not properly treated using unrestricted formalism due to spin contamination problem. However, Chuang et al. [17] showed that the unrestricted quadratic configuration interaction with single and double excitation (UQCISD) even with unrestricted reference states, provides solid approximations to transition state geometries and energies that lead to empirically improved agreement with higher level calculations such as MRCI methods. A greater advantage of the UQCISD with respect to the MRCI method is that vibrational frequencies of the points on the reaction pathway could be computed using analytical energy derivatives. We therefore adopted the UQCI approach in the present study. For the H + HNO reaction, energies and vibrational frequencies along the MEP were also calculated at the UQCISD level of theory in conjunction with the cc-pVTZ basis set. This basis set was optimized to describe dynamical electron correlation effects. The MEP was established in the mass-weighted internal coordinate with a small step size of 0.02 $amu^{1/2}$bohr using the Gonzalez–Schlegel method [18]. Twenty points were automatically selected for Hessian calculations along the MEP by a focusing technique. The energies, vibrational frequencies and moments of inertia of each of these points were used as input for subsequent kinetic calculations employing the variational transition state theory. To reduce the computing cost of calculations for the OH + HNO reaction, we also applied the UQCISD method with the smaller double-zeta (cc-pvDZ) basis set to find the PES. The MEP and the vibrational frequencies and moments of inertia were found by the UMP2/cc-pvDZ and then the energies of each of these points for this reaction were improved by the UQCISD/cc-pVDZ method. All electronic structure calculations were done using the GAUSSIAN 98 program [19].

2.2. Canonical variational transition state theory

Canonical variational transition state theory (CVT) is an extension of transition state theory [20–22]. CVT minimizes the recrossing effects by effectively moving the dividing surface along the MEP between the reactants and products so as to minimize the rate constants. For a canonical ensemble at a given temperature T, the CVT rate constant for a bimolecular reaction is given by

$$k^{\mathrm{CVT}}(T) = \min_s k^{\mathrm{GT}}(T,s), \tag{3}$$

where

$$k^{\mathrm{GT}}(T,s) = \frac{\sigma}{\beta h}\frac{Q^{\mathrm{GT}}(T,s)}{\Phi^{\mathrm{R}}(T)}\mathrm{e}^{-\beta V_{\mathrm{MEP}}(s)}. \tag{4}$$

In these equations, $k^{\mathrm{GT}}(T,s)$ is the generalized transition state theory rate constant at the dividing surface which is orthogonal to the MEP and intersects it at s. σ is the symmetry factor accounting for the possibility of more than one symmetry-related reaction path. In this case, it is one for both reactions (1) and (2). β is $(k_{\mathrm{B}}T)^{-1}$, where k_{B} is Boltzman's constant and h is Planck's constant. $\Phi^{\mathrm{R}}(T)$ is the reactant partition function (per unit volume for bimolecular reactions). $V_{\mathrm{MEP}}(s)$ is the classical potential energy (also called the Born Oppenheimer potential) along the MEP with its zero of energy at the reactants, and $Q^{\mathrm{GT}}(T,s)$ is the internal partition function of the generalized transition state at s with the local zero of energy at $V_{\mathrm{MEP}}(s)$. Both the $\Phi^{\mathrm{R}}(T)$ and $Q^{\mathrm{GT}}(T,s)$ partition functions are approximated as products of electronic, vibrational and rotational partition functions. The relative translational partition function of reactants is also included in Φ^{R}. If the generalized transition state is located at the saddle point ($s = 0$), Eq. (4) reduces to the conventional transition state theory [15]. Since the barriers for reactions (1) and (2) are rather small, quantum mechanical tunneling effects are negligible and thus are not considered.

2.3. Microcanonical variational transition state theory

Microcanonical variational transition state theory (μVT) is based on the idea that by minimizing the microcanonical rate constant $k(E)$ along the MEP, one can minimize the error caused by the 'recrossing' trajectories [23]. Within the framework of μVT, the

thermal rate constant at a fixed temperature T can be expressed as:

$$k^{\mu VT}(T) = \frac{\int_0^\infty \min\{N^{GTS}(E,s)\}e^{-E/k_BT}\,dE}{h\Phi^R}, \quad (5)$$

where $N^{GTS}(E,s)$ is the sum of states of electronic, rotational, and vibrational motions at energy E of the generalized transition state located at s. $N^{GTS}(E,s)$ along the MEP were calculated quantum mechanically using the rigid rotor and harmonic oscillator approximations. Φ^R is a product of electronic, rotational and vibrational partition functions of reactants, and the relative translational partition function of reactants. For the same reason discussed above, quantum transmission effects were not included. All the rate constants were evaluated using our web-based kinetic program VKLab (Virtual Kinetic Laboratory, Web site: http://vklab.hec.utah.edu).

3. Results and discussion

3.1. $H + HNO \rightarrow H_2 + NO$

The potential energy surface of the reaction was calculated using the UQCISD method with the correlation-consistent triplet-zeta basis set (cc-pVTZ) [24]. In particular, the geometry of the abstraction transition state is shown in Fig. 1a. The forward classical barrier height was computed to be 0.5 kcal/mol, which is smaller than the value by Soto et al. [13] but larger than that of Walch [14] mentioned above. The geometry of the transition structure obtained here differs significantly from that derived at the CISD/cc-pVDZ level by Soto, especially the reactive bond distances involved in abstracting the H atom. These differences are indicated in Fig. 1a. Classical and adiabatic potential energy curves along the MEP from UQCISD/cc-pvTZ calculations are shown in Fig. 2. We found that selected points along the MEP have shifted the maximum location to the reactant H + HNO side by −0.074 amu$^{1/2}$ bohr for the classical and by −0.168 amu$^{1/2}$ bohr for the adiabatic potential energy curve.

Rate constants obtained by the CVT and μVT theories at the temperatures from 200 to 2500 K for the forward reaction are listed in Table 1. The fitted Arrhenius expressions for the forward reaction are:

$$k_{1CVT}(T) = 1.608.10^{-12}T^{0.624}e^{-179/T}, \quad (6)$$

$$k_{1\mu VT}(T) = 1.111.10^{-13}T^{0.940}e^{-249/T}. \quad (7)$$

Fig. 3 displays the forward rate constants calculated with both theories along with the available experimental data and previous theoretical results. Fig. 3 also indicates that the present μVT results give a better prediction of rate constants than the CVT in comparison with experimental data. Although Soto et al. [13] also used the CVT theory, the significantly larger rate constants in the present study are due to the lower calculated barrier height in this study, though the differences become smaller as the temperature increases. However, there are some differences between the calculated and experimental data.

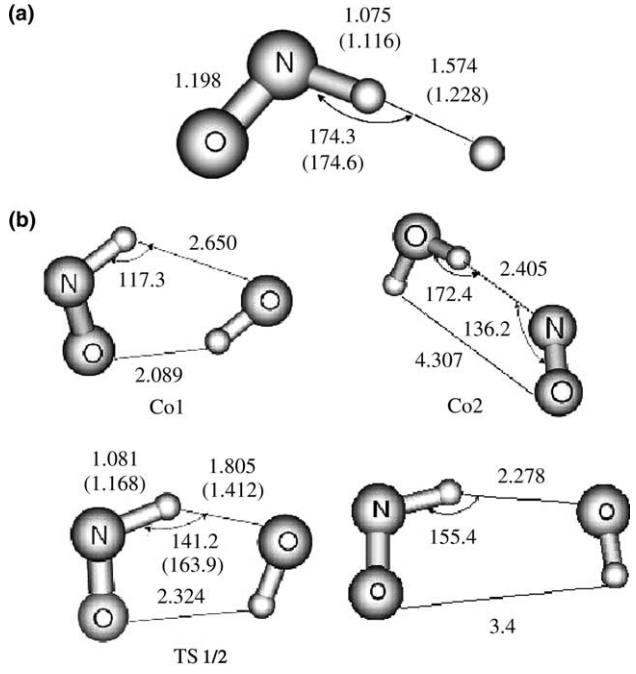

Fig. 1. (a) UQCISD/cc-pvTZ optimized geometries of the saddle point of the H + HNO→H_2 + NO reaction. (b) UQCISD/cc-pvDZ optimized geometries for the saddle point and intermediate complexes of the OH + HNO → H_2O + NO reaction. Soto's results are in the parentheses.

3.2. $OH + HNO \rightarrow H_2O + NO$

The reaction of OH + HNO is a highly exothermic abstraction reaction, and more complicated than the H + HNO. Accordingly, two intermediate complex

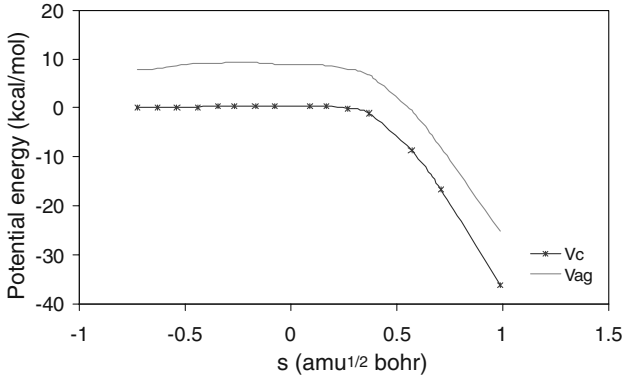

Fig. 2. Plot of UQCISD/cc-pvTZ classical (Vc) and adiabatic (Vag) potential energy along the MEP versus the reaction coordinate s.

Table 1
Calculated CVT and μVT rate constants ($cm^3\,mol^{-1}\,s^{-1}$) for the $H + HNO \rightarrow H_2 + NO$ reaction

Temperatures	CVT	μVT
200	1.57E – 11	5.62E – 12
295	3.55E – 11	9.77E – 12
298	3.56E – 11	9.90E – 12
300	3.57E – 11	9.99E – 12
500	4.94E – 11	1.99E – 11
900	7.60E – 11	4.41E – 11
1000	8.36E – 11	5.10E – 11
1200	1.00E – 10	6.55E – 11
1400	1.19E – 10	8.11E – 11
1600	1.39E – 10	9.78E – 11
1800	1.60E – 10	1.16E – 10
2000	1.83E – 10	1.34E – 10
2100	1.94E – 10	1.44E – 10
2300	2.18E – 10	1.64E – 10
2500	2.43E – 10	1.85E – 10

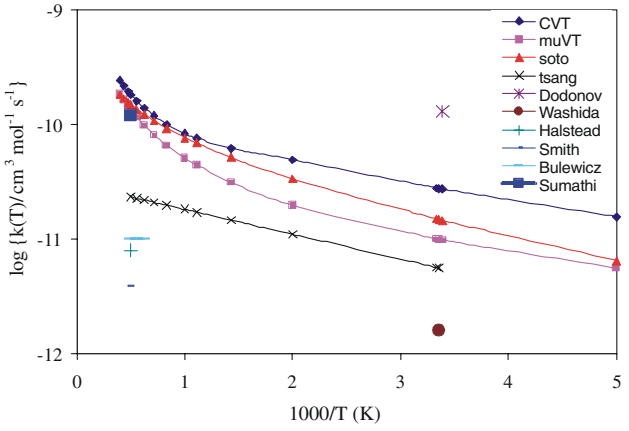

Fig. 3. Arrhenius plots of the present μVT (noted as μVT) and CVT calculated rate constants along with previous theoretical (Soto and Sumathi) and experimental (all the rest) data for the $H + HNO \rightarrow H_2 + NO$ reaction.

structures and a transition state have been located in proceeding from the reactants to products. Fig. 1b shows the optimized geometrical parameters whereas Fig. 4 illustrates a schematic diagram of the relative energies (kcal/mol) of the stationary points on the potential energy surface of OH + HNO at the UQCISD/cc-pvDZ level. Our results of the geometry of the transition structure are significantly different from those of Soto's, especially regarding the two forming and breaking bonds and the angle between them. These differences are shown in Fig. 1b. The energies of all stationary points, including the intermediate HNO(OH) complex (Co1), TS 1/2, NO(H_2O) complex (Co2) and H_2O + NO products, are lower than that of OH + HNO reactants. Thus, there is no barrier for this reaction. In this case, the initial step (i.e., formation of HNO(OH) complex) can be considered as the rate-controlling step of this reaction. In order to calculate the MEP for this reaction, the geometry of a selected point sufficiently far

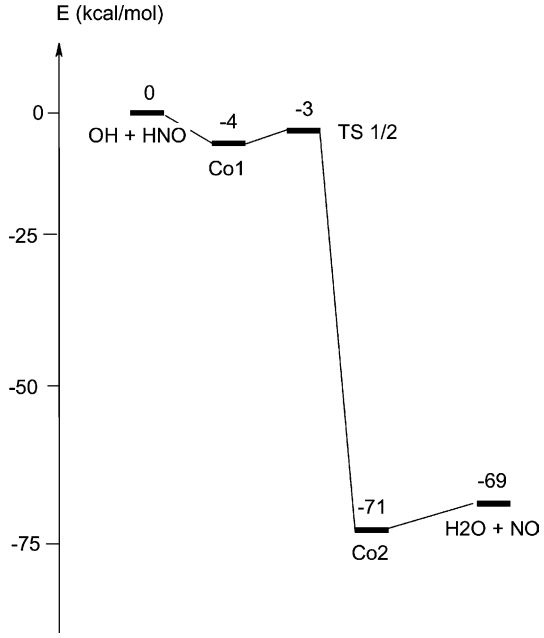

Fig. 4. The potential energy diagram at the UQCISD/cc-pvDZ level for the $OH + HNO \rightarrow H_2O + NO$ reaction.

in the entrance channel was optimized while the active O–H distance was fixed at 3.4 Å and then used as the starting point for a downhill MEP calculation using the UMP2/cc-pVDZ level of theory. Table 2 lists the calculated rate constants obtained by the CVT and μVT theories at the temperatures from 200 to 2500 K for the forward reaction. As noted, our results are quite different from those of Soto et al. [25]. This is due to the fact that in the Soto et al.'s potential energy surface, no intermediate has been located but a barrier height for hydrogen abstraction of 2 kcal/mol has been characterized.

Table 2
Calculated CVT and μVT rate constants ($cm^3\,mol^{-1}\,s^{-1}$) for the $OH + HNO \rightarrow H_2O + NO$ reaction

Temperatures	CVT	μVT
200	1.07E – 11	2.87E – 12
295	1.14E – 11	3.16E – 12
298	1.14E – 11	3.17E – 12
300	1.14E – 11	3.18E – 12
500	1.26E – 11	3.93E – 12
900	1.33E – 11	6.13E – 12
1000	1.44E – 11	6.90E – 12
1200	1.72E – 11	8.75E – 12
1400	2.08E – 11	1.10E – 11
1600	2.50E – 11	1.37E – 11
1800	3.00E – 11	1.69E – 11
2000	3.58E – 11	2.06E – 11
2100	3.89E – 11	2.26E – 11
2300	4.57E – 11	2.71E – 11
2500	5.33E – 11	3.20E – 11
2500	5.33E – 11	3.20E – 11

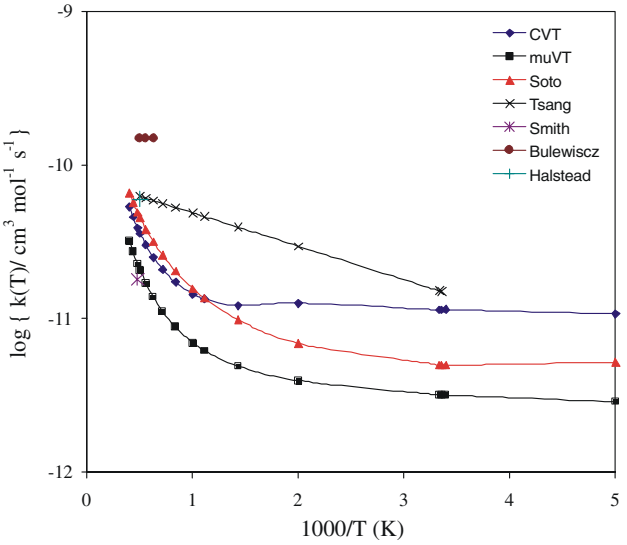

Fig. 5. Arrhenius plot of the present μVT (noted as μVT) and CVT calculated rate constants along with previous theoretical (Soto) and experimental (all the rest) results for the $OH + HNO \rightarrow H_2O + NO$ reaction.

The fitted Arrhenius expressions for the forward reaction are as follows:

$$k_{2CVT}(T) = 2.191.10^{-14} T^{0.943} e^{-239/T}, \quad (8)$$

$$k_{2\mu VT}(T) = 1.996.10^{-15} T^{1.189} e^{-168/T}. \quad (9)$$

Fig. 5 displays the calculated forward rate constants with both of the above expressions, as well as the available experimental data and previous theoretical results by Soto et al. [25]. The calculated abstraction rate constant using μVT is in agreement with the experimental determination of Smith [9] at 2100 K but the CVT results turn out to be closer to those reported by Tsang et al. [12].

4. Conclusions

In summary, in this theoretical work, we have carried out a direct ab initio dynamics study of the two hydrogen abstraction reactions between H and OH with HNO using the UQCISD level of theory. The calculated classical barrier height of the H + HNO reaction amounts to 0.5 kcal/mol, which is smaller than the earlier theoretical result by Soto et al. [13] but larger than that of Walch [14]. The OH + HNO reaction is characterized as a barrierless process and proceeds via two weakly-bonded complexes, in contrast to the Soto's results showing a barrier of 2 kcal/mol. The geometries of transition state structures obtained in the present work also differ markedly from those reported by Soto.

The rate constants of hydrogen abstraction reactions H + HNO and OH + HNO evaluated using both μVT and CVT theories can be expressed as follows:

$$k_{1CVT}(T) = 1.608.10^{-12} T^{0.624} e^{-179/T},$$

$$k_{1\mu VT}(T) = 1.111.10^{-13} T^{0.940} e^{-249/T}$$

and

$$k_{2CVT}(T) = 2.191.10^{-14} T^{0.943} e^{-239/T},$$

$$k_{2\mu VT}(T) = 1.996.10^{-15} T^{1.189} e^{-168/T},$$

respectively.

Due to a difference in the barrier heights, the present calculated $k_{1CVT}(T)$ and $k_{2CVT}(T)$ values also deviate appreciably from the CVT results by Soto et al. The μVT result for the $H + HNO \rightarrow H_2 + NO$ reaction is closer to the available experimental data than the CVT counterparts. For the OH + HNO reaction, our results obtained from the μVT treatment are closer to the values of Smith [9], whereas the rate constants evaluated by the CVT theory are in better agreement with the values of Tsang et al. [12]. Since the OH + HNO reaction is a barrier-free process, the μVT results are expected to be more accurate. Overall, we would suggest that further experiments reexamining the kinetics of these basic reactions are highly desirable.

Acknowledgements

This work has been supported by the University of Utah Center for the Simulation of Accidental Fires&Explosions, funded by the Department of Energy, Lawrence Livermore National Laboratory, under subcontract B341493 and a generous gift from Dow Chemical Company. The authors thank the Utah Center for High Performance Computing for computer time. The Leuven group, MTN, JP and HMTN, thanks the Flemish Fund for Scientific Research (FWO-Vlaanderen) and the K.U. Leuven Research Council (GOA program) for continuing support.

References

[1] E.M. Bulewicz, T.M. Sugden, Proc. Roy. Soc. (London) A 277 (1964) 43.
[2] E.A. Albers, K. Hoyermann, H.G. Wagner, J. Wolfrum, in: Proceedings of the 12th International Symposium on Combustion, 1969, p. 313.
[3] A.M. Dean, I.E. Hardy, R.K. Lyon, in: Proceedings of the 19th International Symposium on Combustion, 1982, p. 97.
[4] A.M. Dean, M.S. Chou, D. Stern, ACS Symp. 249 (1984) 71.
[5] S.L. Chen, J.A. Cole, M.P. Heap, J.C. Kramlich, J.M. McCarthy, D.W. Preshing, in: Proceedings of the 22nd International Symposium on Combustion, 1988, p. 1135.

[6] Xu, Minghou, Fan, Yaoguo, Yuan, Jianwei, Sheng, Changdong, Yao, Hong, Int. J. Energy Res., vol. 23, 1999, p. 683.
[7] S.L. Chen, J.A. Cole, M.P. Heap, J.C. Kramlich, J.M. McCarthy, D.W. Pershing, in: Proceedings of the 22nd International Symposium Combustion, 1988, p. 1135.
[8] C.J. Halstead, D.R. Jenkins, Chem. Phys. Lett. 2 (1968) 281.
[9] M.Y. Smith, Combust. Flame 293 (1972) 293.
[10] N. Washida, H. Akimoto, M. Okuda, J. Phys. Chem. 82 (1978) 2293.
[11] A.F. Dodonov, V.V. Zelenov, V.P. Strunin, V.L. Tal'roze, Kinet. Catal. 22 (1981) 689.
[12] W. Tsang, J.T. Herron, J. Phys. Ref. Data 20 (1991) 609.
[13] M.R. Soto, M. Page, J. Chem. Phys. 97 (1992) 7287.
[14] S.P. Walch, J. Chem. Phys. 99 (1993) 3804.
[15] R. Sumathy, S. Debasis, M.T. Nguyen, J. Phys. Chem. A 102 (18) (1998) 3175.
[16] T.N. Truong, Wendell T. Duncan, Robert L. Bell, Direct Ab initio dynamics methods for calculating thermal rates of polyatomic reactions, in: B.B. Laird, R. Ross, T. Ziegler (Eds.), ACS Symposium Series Volume on Density Functional Theory in Chemistry, Anaheim, CA on April 2–6, 1995.
[17] Y.-Y. Chuang, E.L. Coitino, D.G. Truhlar, J. Phys. Chem. A 104 (2000) 446.
[18] C. Gonzalez, H.B. Schlegel, J. Phys. Chem. 94 (1990) 5523.
[19] M.J. Frisch et al., GAUSSIAN 98, Gaussian Inc., Pittsburgh, PA, 1998.
[20] B.C. Garrett, D.G. Truhlar, J. Chem. Phys. 70 (1979) 1593.
[21] D.G. Truhlar, B.C. Garrett, Acc. Chem. Rev. 13 (1980) 440.
[22] S.C. Tucker, D.G. Truhlar, in: J. Bertran, I.G. Csizmadia (Eds.), New Theoretical Concepts for Understanding Organic Reactions, Kluwer, Dordrecht, The Nertherlands, 1989, p. 291.
[23] S. Zhang, Thanh N. Truong, J. Chem. Phys. 113 (2000) 6149.
[24] T.H. Dunning Jr, J. Chem. Phys. 90 (1989) 1007.
[25] M.R. Soto, M. Page, M.L. McKee, Chem. Phys. 153 (1991) 415.